Murine Coronavirus Mouse Hepatitis Virus Is Recognized by MDA5 and Induces Type I Interferon in Brain Macrophages/Microglia[▽]

Jessica K. Roth-Cross, Susan J. Bender, and Susan R. Weiss*

Department of Microbiology, University of Pennsylvania School of Medicine, Philadelphia, Pennsylvania 19104

The coronavirus mouse hepatitis virus (MHV) induces a minimal type I interferon (IFN) response in several cell types in vitro despite the fact that the type I IFN response is important in protecting the mouse from infection in vivo. When infected with MHV, mice deficient in IFN-associated receptor expression (IFNAR$^{-/-}$) became moribund by 48 h postinfection. MHV also replicated to higher titers and exhibited a more broad tissue tropism in these mice, which lack a type I IFN response. Interestingly, MHV induced IFN-β in the brains and livers, two main targets of MHV replication, of infected wild-type mice. MHV infection of primary cell cultures indicates that hepatocytes are not responsible for the IFN-β production in the liver during MHV infection. Furthermore, macrophages and microglia, but not neurons or astrocytes, are responsible for IFN-β production in the brain. To determine the pathway by which MHV is recognized in macrophages, IFN-β mRNA expression was quantified following MHV infection of a panel of primary bone marrow-derived macrophages generated from mice lacking different pattern recognition receptors (PRRs). Interestingly, MDA5, a PRR thought to recognize primarily picornaviruses, was required for recognition of MHV. Thus, MHV induces type I IFN in macrophages and microglia in the brains of infected animals and is recognized by an MDA5-dependent pathway in macrophages. These findings suggest that secretion of IFN-β by macrophages and microglia plays a role in protecting the host from MHV infection of the central nervous system.

The type I interferon (IFN) response, consisting of IFN-α/β, represents one of the first lines of defense against viral infection. During viral infection of a cell, pathogen-associated molecular patterns, such as double-stranded RNA (dsRNA), are exposed and recognized by pattern recognition receptors (PRRs). These PRRs include Toll-like receptors (TLRs), such as TLR3, that reside on the cell membrane or in endosomal compartments and the cytoplasmic receptors RIG-I (retinoic acid-inducible gene I) and MDA5 (melanoma differentiation-associated protein 5) (8). Recognition by PRRs leads to the activation of IRF-3 (IFN regulatory factor 3), which dimerizes and translocates to the nucleus. In the nucleus it associates with the promoter region of the IFN-β gene along with NF-κB, AP-1, and CBP/p300, driving IFN-β transcription. Once IFN-β is produced, it is secreted from infected cells and is able to bind to the IFN-associated receptor (IFNAR) on neighboring cells, amplifying the production of IFN-β and inducing the expression of IFN-α and many IFN-stimulated genes (37, 41). This series of events generates an antiviral milieu that helps to limit viral spread. Therefore, it is not surprising that many viruses have developed mechanisms to subvert or alter the type I IFN response, making it more difficult for the host to combat viral infection (8, 20).

Mouse hepatitis virus (MHV), a group 2 coronavirus (CoV), is a positive-strand RNA virus. Depending on the strain, MHV can infect both the brain and the liver and cause both acute and chronic disease of various degrees of severity. Therefore, it is used as a model for viral hepatitis, viral encephalitis, and demyelinating diseases such as multiple sclerosis (51). While little is yet known about how MHV induces and responds to a type I IFN response in vivo (16, 39, 40, 60), recent data have begun to shed light on the complex interactions between MHV and the IFN response in vitro. Several studies have shown that MHV is a poor inducer of type I IFN in vitro (7, 47, 48, 57, 58) and induces IFN-β mRNA only late during infection of mouse fibroblast cells (40). However, MHV is able to induce IFN-α in plasmacytoid dendritic cells (pDCs), the major IFN-producing cells in vivo (7). MHV also employs several mechanisms to subvert the type I IFN response in vitro. MHV does not induce the production of IFN-β protein (40) and is resistant to the antiviral effects of IFN-β in vitro (40, 45, 52, 58), suggesting that it can alter IFN signaling or its downstream effects. More specifically, MHV nucleocapsid (N) protein has been shown to inhibit RNase L activity, a downstream effect of type I IFN signaling (52), and the nsp1 protein of MHV has been reported to also play a role in interfering with the type I IFN response (60). Interestingly, the N protein of severe acute respiratory syndrome (SARS-CoV), a related CoV, is able to inhibit type I IFN synthesis, and the proteins encoded by Orf3 and Orf6 inhibit both type I IFN synthesis and signaling (22). In addition, the nsp1 protein of SARS induces mRNA degradation in infected cells, preventing the accumulation of IFN-β mRNA (17), and inhibits type I IFN signaling by decreasing STAT1 phosphorylation (50).

We have further investigated the pathway by which MHV induces type I IFN and the cell types that produce type I IFN during viral infection in vivo. We demonstrate that macrophages and macrophage-like microglia produce IFN-β in the brains of MHV-infected animals and that, in macrophages, MHV induces type I IFN by an MDA5-dependent pathway.

---

* Corresponding author. Mailing address: Department of Microbiology, University of Pennsylvania, School of Medicine, 36th Street and Hamilton Walk, Philadelphia, PA 19104-6076. Phone: (215) 898-8013. Fax: (215) 573-4858. E-mail: weisssr@mail.med.upenn.edu.

MATERIALS AND METHODS

Viruses. Recombinant RA59 (RA59) (34), recombinant RJHM (RJHM) (31), MHV-2 (43), and MHV-3 (49) have been described previously. Sendai virus (SeV) Cantell strain (3) and Newcastle disease virus expressing green fluorescent protein (NDV-GFP) (33) were provided by Adolfo García-Sastre (Mount Sinai School of Medicine, New York, NY), and Sindbis virus expressing GFP (5) was provided by Sara Cherry (University of Pennsylvania, Philadelphia, PA). Lysate from 17Cl1 mouse fibroblast cells was used in mock infections.

Mice. Virus-free C57BL/6 mice were purchased from the National Cancer Institute (Frederick, MD) and 129x1/SvJ mice were purchased from Jackson Laboratories (Bar Harbor, ME). IFNAR$^{-/-}$ interleukin-12 receptor (IL-12R)$^{+/-}$ mice and IL-12R$^{+/-}$ mice, both on a C57BL/6 background, were provided by Hao Shen (University of Pennsylvania, Philadelphia, PA). IFNAR$^{-/-}$ IL-12R$^{+/-}$ mice are referred to below as IFNAR$^{-/-}$ mice.

Infection of IFNAR$^{-/-}$ mice. Four- to five-week-old IFNAR$^{-/-}$, IL-12R$^{+/-}$, and wild-type (WT) C57BL/6 mice were infected by intracranial (i.c) inoculation with 500 PFU of RA59 or 10 PFU of RJHM virus. At 2 days postinfection (p.i.), animals were sacrificed, and brains, livers, spleens, lungs, kidneys, hearts, stomachs, and intestines were harvested and placed in isotonic saline containing 0.167% gelatin (gel saline) and homogenized. Viral titers were determined by plaque assay on L2 fibroblasts (11).

IFN-β expression in the brain and liver. To measure IFN-β mRNA and protein expression in the brains of infected mice, 3- to 4-week-old C57BL/6 mice were infected by i.c. inoculation with 50 PFU of RA59 or RJHM virus and brains were harvested at 5 days p.i. To measure IFN-β expression levels in the liver, 3- to 4-week-old C57BL/6 mice were infected by intrahepatic (i.h.) inoculation with 500 PFU of RA59, RJHM, MHV-2, or MHV-3, and livers were harvested at 3 days p.i. RNA was isolated from brains and livers as previously described (40). IFN-β mRNA levels in the brain were measured by real-time quantitative PCR (qPCR), using a custom-designed low-density array card in collaboration with Centocor Inc. (Radnor, PA). IFN-β mRNA levels in the liver were measured by real-time qPCR with primers specific for the IFN-β gene (40). Cycle threshold (C_T) values were normalized to 18S rRNA levels, resulting in a ΔC_T value [$\Delta C_T = C_{T(IFN-\beta)} - C_{T(18S)}$]. $\Delta\Delta C_T$ values were calculated [$\Delta\Delta C_T = \Delta C_{T\,(infected)} - \Delta C_{T(mock)}$], and all results are expressed as relative change over the value in mock-infected animals ($2^{-\Delta\Delta C_T}$).

IFN-β protein levels in tissue and cells. To measure IFN-β protein, flash-frozen tissues were homogenized in cold phosphate-buffered saline supplemented with Complete protease inhibitors (Roche Applied Science). Protein samples were diluted to 1 mg/ml total protein, and IFN-β protein levels were measured using a mouse IFN-β enzyme-linked immunosorbent assay (ELISA) kit (PBL Biomedical Laboratories). IFN-β protein levels in infected animals are normalized to protein levels in mock-infected animals. IFN-β protein in primary hepatocyte culture supernatants was measured by IFN-β ELISA (PBL Biomedical Laboratories) as per the manufacturer's instructions.

Generation of primary hepatocyte cultures. Primary hepatocyte cultures were generated from 8- to 10-week-old C57BL/6 mice. Mice were anesthetized with 2,2,2-tribromoethanol (Avertin), and livers were perfused and digested in situ through the portal vein with liver perfusion medium (Invitrogen) and liver digestion medium (Invitrogen), respectively. Tissue was dissociated further by mechanical disruption through nylon mesh and centrifuged through 45% Percoll. Hepatocytes were cultured on BioCoat collagen I-coated plates (BD Biosciences) in RPMI 1640 medium containing 10% fetal bovine serum (FBS). After 1 day in culture, hepatocytes were inoculated with 2 PFU/cell of RA59, RJHM, MHV-2, MHV-3, or SeV.

Generation of brain-derived primary cell cultures. Primary hippocampal neuron cultures were prepared from embryonic day 15 to 16 C57BL/6 mice (35) and cultured in neurobasal medium supplemented with B27 supplement (Invitrogen), 100 U/ml penicillin, 100 ng/ml streptomycin, 2 mM L-glutamine, and 4 μg/ml glutamate in the absence of an astrocyte feeder layer. Cells were cultured for 4 days prior to infection with MHV and were approximately 90 to 95% pure, as determined by positive immunostaining for microtubule-associated protein 2 (data not shown). Neuron cultures were inoculated with 5 PFU/cell of RA59 or RJHM or 50 PFU/cell of GFP-expressing Sindbis virus.

Primary astrocyte cultures were generated from the brains of 1- to 3-day-old neonatal C57BL/6 mice. Tissue was dissociated by mechanical disruption through nylon mesh and plated in complete medium consisting of minimal essential medium supplemented with 10% FBS, 1% nonessential amino acid solution, 2 mM L-glutamine, 50 U/ml penicillin, 50 μg/ml streptomycin, and 10 mM HEPES. After 5 days in culture, flasks were shaken to remove nonadherent cells, and remaining adherent cells were ≥95% pure astrocytes, as determined by positive immunostaining for glial fibrillary acidic protein (data not shown).

Primary microglia cultures were generated from neonatal mice similarly to astrocyte cultures. However, cells were plated in complete medium consisting of Dulbecco's modified Eagle's medium supplemented with 10% FBS, 2 mM L-glutamine, 50 U/ml penicillin, and 50 μg/ml streptomycin. After 12 days in culture, flasks were shaken at 200 rpm for 45 min to remove nonadherent cells including microglia. Cells were plated, and 30 min later, medium was replaced to remove any floating cells. Microglia cultures were ≥95% pure as determined by positive immunostaining for CD11b and negative staining for glial fibrillary acidic protein (data not shown). Astrocyte and microglia cultures were infected with 1 PFU/cell of RA59, RJHM, or SeV.

Generation of primary macrophage cultures. Primary bone marrow-derived macrophages (BMM) were isolated as previously described (6) from the hind limbs of 6- to 8-week-old C57BL/6, 129x1/SvJ, RIG-I$^{-/-}$, MyD88$^{-/-}$, TLR3$^{-/-}$, and MDA5$^{-/-}$ mice. Hind limbs from MDA5$^{-/-}$ (129x1/SvJ background) (10) and TLR3$^{-/-}$ (C57BL/6 background) (2) mice were provided by Michael Diamond (Washington University in St. Louis, St. Louis, MO), hind limbs from MyD88$^{-/-}$ (C57BL/6 background) mice (1) were provided by Larry Turka (University of Pennsylvania, Philadelphia, PA), and hind limbs from RIG-I$^{-/-}$ (ICR × 129x1/SvJ × C57BL/6 background) mice (19) were provided by Michael Gale (University of Washington School of Medicine, Seattle, WA). Macrophages were cultured in macrophage medium consisting of Dulbecco's modified Eagle's medium supplemented with 10% FBS, 20% L cell-conditioned medium, 1 mM sodium pyruvate, 100 U/ml penicillin, 100 μg/ml streptomycin, and 25 mM HEPES. Cells were harvested 7 days after plating and were ≥99% pure (CD11b$^+$ CD11c$^-$), as determined by surface straining followed by flow cytometry (data not shown). BMM cultures were infected with 0.5 PFU/cell of RA59, RJHM, or SeV.

Real-time qPCR analysis of primary cell culture RNA. RNA was isolated from primary cell cultures 24 h p.i. using an RNeasy mini kit (Qiagen), and IFN-β transcript levels were determined by real-time qPCR as previously described (40). mRNA7 levels were measured using the following primers: F, 5′-TATAA GAGTGATTGGCGTCC-3′; R, 5′GAGTAATGGGGAACCACACT-3′. All real-time PCR data are expressed as the relative change over values in mock-infected animals as described above.

Intracellular IFN-β staining and flow cytometric analysis. Primary BMM cultures were inoculated with 0.5 PFU/cell of RA59 or RJHM and harvested at 24 h p.i. Brain-derived mononuclear cells were isolated at day 5 p.i. from mice infected with 5,000 PFU of RA59 or 10 PFU of RJHM virus or mock infected. Brains were homogenized, and cells were passaged through 35% Percoll onto a 70% Percoll cushion. Fc receptors were blocked prior to staining. Cells were then stained for surface expression of CD45 and CD11b. Macrophages were characterized by high surface expression of CD11b and CD45 (CD11b^{hi} CD45^{hi}), while microglia were characterized by intermediate expression of CD11b and CD45 (CD11b^{int} CD45^{int}). After surface staining, cells were fixed and permeabilized with the Cytofix/Cytoperm kit (PharMingen), and intracellular IFN-β was detected with a fluorescein isothiocyanate-conjugated rat anti-mouse IFN-β antibody (clone RMMB-1; PBL Biomedical Laboratories). Data were collected using a FACSCalibur flow cytometer (Becton Dickinson) and analyzed using FlowJo software (Tree Star, Inc.).

IFN-β bioassay. Supernatants from BMM infected with 0.5 PFU/cell of RA59, RJHM, or SeV were exposed to 6,000 J/m^2 UV light in a Stratalinker 1800 (Stratagene) to inactivate the virus. L2 mouse fibroblast cells were treated with the UV-inactivated supernatants for 24 h and then infected with 1 PFU/cell of NDV-GFP. At 24 h p.i., cells were examined under a Nikon Eclipse 2000E-U fluorescence microscope.

RESULTS

MHV replication is accelerated, and tissue tropism is extended in mice with a defective type I IFN response. Replication of many viruses is restricted by the type I IFN response in vivo, limiting it to specific tissues (15, 28, 29, 42). To examine if the type I IFN response restricts MHV replication in vivo, WT C57BL/6 mice and IFNAR$^{-/-}$ mice were infected i.c. with either the RA59 or the RJHM strain of MHV. These are recombinant versions of two prototypic MHV strains. RA59 is dual tropic, infecting the brain and the liver, while RJHM is a highly neurotropic strain, restricted to replication in the brain (51). MHV-infected IFNAR$^{-/-}$ mice were moribund by day 2 p.i., consistent with previous results (7). Therefore, viral
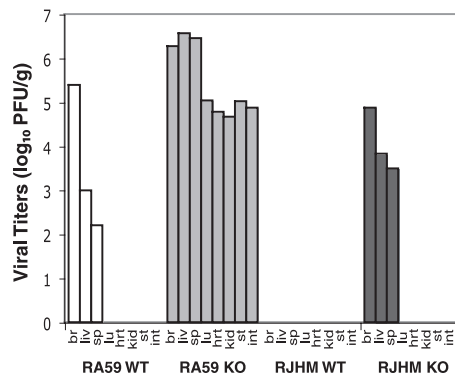
FIG. 1. MHV replication in IFNAR-deficient mice. WT C57BL/6 or IFNAR$^{-/-}$ (KO) mice were infected i.c. with either 500 PFU of RA59 or 10 PFU of RJHM. At 2 days p.i., mice were sacrificed, and viral titers in the brain (br), liver (liv), spleen (sp), lung (lu), heart (hrt), kidney (kid), stomach (st), and intestines (int) were determined by plaque assay on L2 cells. Data shown are averages of two mice per group and are derived from one representative experiment of two.
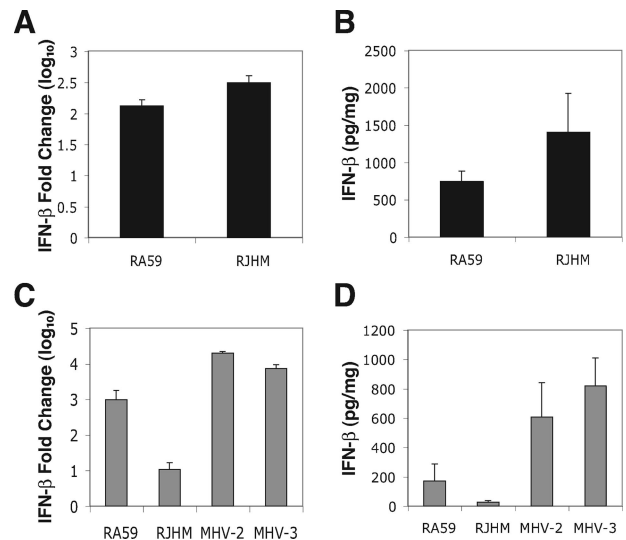

FIG. 2. IFN-β induction in the brain and liver of MHV-infected mice. (A and B) C57BL/6 mice were infected with 50 PFU of RA59 or RJHM or mock-infected by i.c. inoculation. (A) RNA was isolated from brains at day 5 p.i. (RA59, $n = 9$; RJHM, $n = 6$; mock, $n = 10$), and IFN-β mRNA was measured by real-time qPCR. (B) Total protein was isolated from brains of infected mice at day 5 p.i. (RA59, $n = 5$; RJHM, $n = 2$; mock, $n = 5$), and IFN-β protein levels were measured using a mouse IFN-β ELISA. Data from panel A and B represent averages from two independent experiments and are re-plotted from Roth-Cross et al. (35). (C and D) C57BL/6 mice were infected with 500 PFU of RA59, RJHM, MHV-2, or MHV-3 or mock-infected by i.h. inoculation. (C) IFN-β mRNA and (D) IFN-β protein levels in livers at day 3 p.i. (RA59, $n = 5$; RJHM, $n = 5$; MHV-2, $n = 3$; MHV-3, $n = 4$; mock, $n = 5$). IFN-β mRNA data are represented as relative induction over mock-infected animals. IFN-β protein data are normalized by subtraction of IFN-β protein levels in mock-infected animals (IFN-β$_{infected}$ − IFN-β$_{mock}$). Error bars represent the standard error of the mean, and data are derived from one representative experiment of two.

replication and spread were assessed at 48 h p.i. by quantifying viral titers in organs of infected WT C57BL/6 and IFNAR$^{-/-}$ mice. As expected, RA59 was detected in the brains, livers, and spleens of infected WT C57BL/6 mice (Fig. 1, RA59 WT). In contrast, infection of IFNAR$^{-/-}$ mice with RA59 led to increased levels of viral replication in all organs examined (Fig. 1, RA59 KO). Similar results were obtained with RJHM. While virus was not detectable in any organs tested from RJHM-infected WT C57BL/6 mice at day 2 p.i. (Fig. 1, RJHM WT), RJHM was detected in the brains, livers, and spleens of RJHM-infected IFNAR$^{-/-}$ mice (Fig. 1, RJHM KO). Thus, the type I IFN response plays an important role in early restriction of MHV replication and tissue tropism.

MHV induces IFN-β in brains and livers of infected animals. Since the type I IFN response limits viral replication and spread of MHV in vivo, we investigated whether MHV induces a type I IFN response in the two main targets of replication in C57BL/6 mice, the brain and the liver. To examine the type I IFN response in the brains of infected animals, WT C57BL/6 mice were infected i.c. with either RA59 or RJHM. At 5 days p.i., the peak of viral replication, IFN-β mRNA levels were assessed by real-time qPCR (Fig. 2A). Both RA59 and RJHM induced IFN-β mRNA levels to 10^2- to 10^3-fold over that in mock-infected animals. This is consistent with previous studies that show that MHV induces IFN-β mRNA in the brains of infected animals (38, 39). To measure IFN-β protein levels in the brains of infected animals at day 5 p.i., total protein was isolated, and IFN-β protein was quantified by ELISA (Fig. 2B). As expected from the levels of IFN-β mRNA, both RA59 and RJHM induced measurable levels of IFN-β protein in the brain. It should be noted that IFN-β protein levels were below the level of detection in mock-infected brains.

In order to measure the levels of type I IFN in the livers of infected animals, WT C57BL/6 mice were infected i.h. with RA59, RJHM, or one of the highly hepatotropic strains, MHV-2 and MHV-3. IFN-β mRNA levels in the liver were measured at day 3 p.i. by real-time qPCR using primers specific to the IFN-β gene (Fig. 2C). As animals infected with MHV-2 and MHV-3 died prior to day 5, samples were analyzed at day

3 p.i. instead of day 5 p.i. Similar to what was observed for IFN-β expression in the brain, MHV induced IFN-β mRNA in the liver, with the highly hepatotropic strains of MHV inducing significantly higher levels of IFN-β mRNA ($P < 0.05$). Notably, RJHM, which replicates very poorly in the liver (31), induced little to no IFN-β mRNA (Fig. 2C). IFN-β protein levels, quantified by ELISA from total liver protein isolated from infected animals, corresponded to IFN-β mRNA levels, with RJHM inducing little to no IFN-β protein and RA59, MHV-2, and MHV-3 inducing measurable levels of IFN-β protein (Fig. 2D). Together, these data indicate that while the type I IFN response prevents spread of MHV to organs such as the kidneys and heart, MHV is able to replicate and induce IFN-β in both the brains and livers of infected animals.

MHV does not induce IFN-β in primary hepatocyte cultures. To determine which cell types produce type I IFN during MHV infection of the liver, primary hepatocyte cultures were derived from WT C57BL/6 mice. Hepatocytes were infected with RA59, RJHM, MHV-2, or MHV-3. At 24 h p.i. RNA was isolated from infected cells, and IFN-β mRNA induction was quantified by real-time qPCR (Fig. 3A). IFN-β induction by SeV was used as a control for the ability of primary hepatocyte cultures to produce IFN-β during viral infection. While SeV
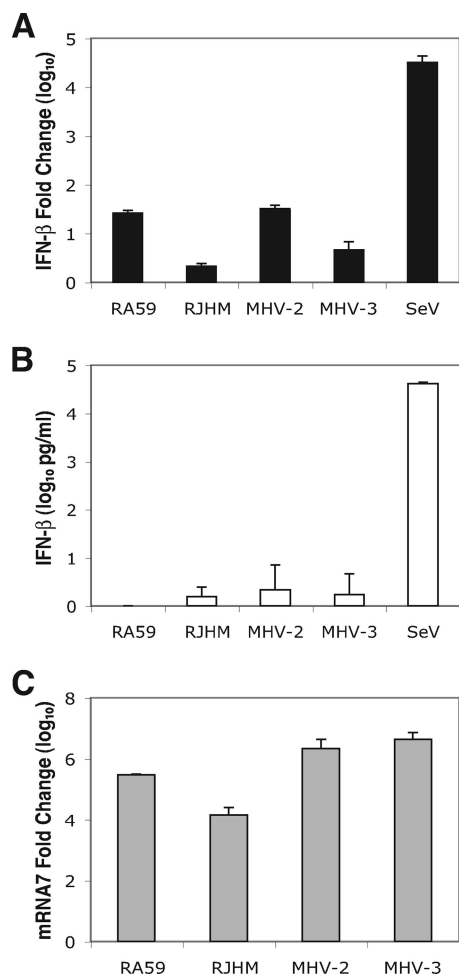
FIG. 3. IFN-β induction in MHV-infected primary hepatocyte cultures. Primary hepatocyte cultures were infected with 2 PFU/cell of RA59, RJHM, MHV-2, MHV-3, or SeV or mock infected. At 24 h p.i., whole-cell RNA was isolated and IFN-β mRNA (A) and mRNA7 levels (C) were quantified by real-time qPCR. (B) At 24 h p.i., total released IFN-β protein was measured by ELISA (limit of detection is 15.6 pg/ml). Real-time qPCR data are represented as relative induction over mock-infected cells. IFN-β protein data are normalized by subtraction of IFN-β protein levels in mock-infected cells (IFN-$\beta_{infected}$ − IFN-β_{mock}). Error bars represent the standard error of the mean of three replicates, and data are derived from one representative experiment of three.

induced high levels of IFN-β mRNA, none of the MHV strains examined induced significant amounts of IFN-β mRNA. Similar results were seen at 48 h p.i. (data not shown). Since there was only a low level of IFN-β mRNA detected, we determined whether this mRNA was sufficient for IFN-β protein production. Supernatants from infected cells were subjected to ELISA to quantify IFN-β protein levels (Fig. 3B). However, none of the MHV strains examined induced IFN-β protein to levels over the limit of detection (15.6 pg/ml, as per the manufacturer), while SeV induced ample amounts of IFN-β protein.

To ensure that the lack of an IFN response to MHV was not due to the inability of MHV to replicate in primary hepatocyte cultures, mRNA7 levels were measured by real-time qPCR

(Fig. 3C). mRNA7, which encodes the N gene, is the most abundant subgenomic mRNA generated during MHV replication (44) and is thus used as a measure of the level of MHV replication. RA59, MHV-2, and MHV-3 replicated well in primary hepatocyte cultures, as determined by induction of mRNA7 transcription. Interestingly, RJHM also induced high levels of mRNA7 transcription in primary hepatocyte cultures even though it was unable to establish an infection in the livers of infected animals. Thus, although MHV is able to replicate in primary hepatocyte cultures, it does not induce a type I IFN response. Therefore, it is unlikely that hepatocytes represent the major IFN-producing cells in the livers of infected animals.

MHV induces IFN-β in primary microglial cultures but not in primary neuron or astrocyte cultures. To determine which cells are responsible for producing type I IFN in the brains of MHV-infected animals, primary hippocampal neuron cultures were derived from WT C57BL/6 embryonic mice, and primary astrocyte and microglial cultures were derived from WT C57BL/6 neonatal mice. Cultures were infected with RA59 or RJHM, RNA was isolated at 24 h p.i., and IFN-β mRNA levels were quantified by real-time qPCR (Fig. 4). In addition, primary neuron cultures were infected with Sindbis virus, a virus known to infect neurons in vivo, and primary astrocyte and mixed glial cultures were infected with SeV to serve as positive controls for type I IFN induction. While Sindbis virus induced high levels of IFN-β mRNA in primary neuron cultures, neither RA59 nor RJHM induced a type I IFN response (Fig. 4A). Similarly, RA59 and RJHM induced minimal levels of IFN-β mRNA in primary astrocyte cultures compared to SeV (Fig. 4C). To ensure that the lack of IFN-β induction was not due to the inability of MHV to replicate in primary neuron and astrocyte cultures, mRNA7 levels were measured by real-time qPCR. RA59 and RJHM induced significant levels of mRNA7 transcript in both primary neuron (Fig. 4B) and astrocyte (Fig. 4D) cultures, indicating that MHV can replicate in these cells (26, 35).

Both RA59 and RJHM induced IFN-β mRNA to levels comparable to SeV in primary microglial cultures (Fig. 4E). Consistent with previous observations (26), MHV was also able to replicate in microglial cultures (Fig. 4F). It should be noted that, although it is unlikely, the presence of a small percentage of oligodendrocytes could not be discounted. Thus, the data in Fig. 4 demonstrate that microglia, but not neurons or astrocytes, produce type I IFN in the brains of MHV-infected animals.

Macrophages and microglia produce IFN-β in response to MHV infection. Since microglia are macrophage-like cells, we investigated the ability of MHV to induce a type I IFN response in another macrophage cell population. To this end, primary BMM cultures were derived from WT C57BL/6 mice. BMM were infected with RA59, RJHM, or SeV as a positive control for IFN induction. RNA was isolated at 24 h p.i. and used to measure IFN-β mRNA levels by real-time qPCR (Fig. 5A). Similar to what was observed in microglial cultures, MHV induced IFN-β mRNA in BMM. However, in these cells, MHV induced IFN-β mRNA to levels significantly higher than SeV in BMM ($P < 0.05$). To determine if MHV induced IFN-β protein production in BMM, cells were stained for intracellular IFN-β and analyzed by flow cytometry (Fig. 5B). Infection with either RA59 or RJHM resulted in a shift in the mean fluores-

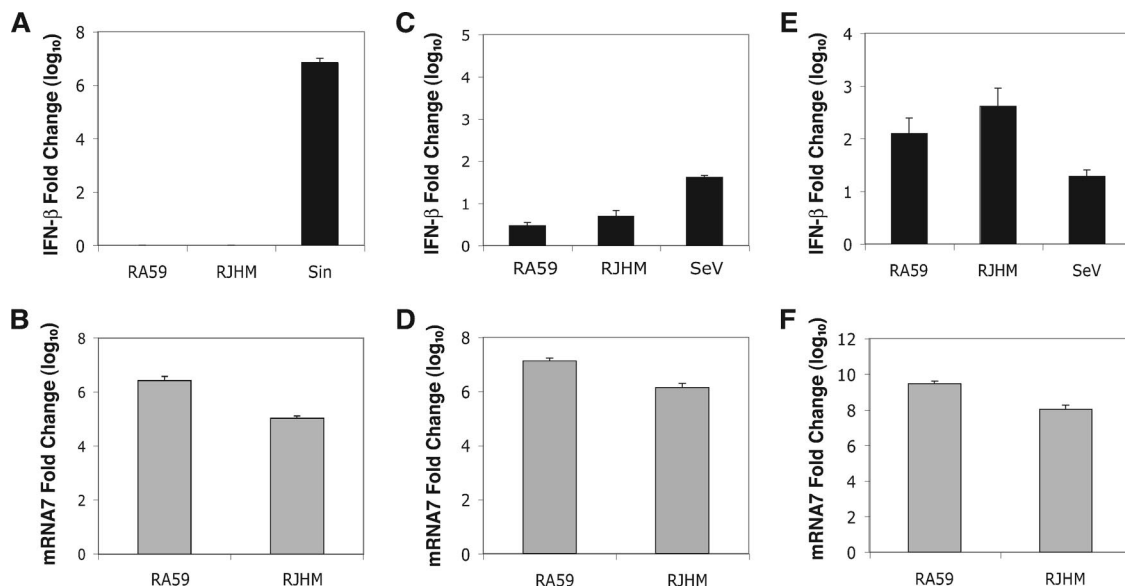FIG. 4. IFN-β induction in MHV-infected brain-derived primary cell cultures. (A and B) Primary hippocampal neuron cultures were infected with 5 PFU/cell of RA59 or RJHM or 50 PFU/cell of Sindbis (Sin) virus or mock infected. At 24 h p.i., whole-cell RNA was isolated, and IFN-β mRNA (A) and mRNA7 (B) levels were measured by real-time qPCR. Primary astrocyte cultures (C and D) and primary mixed glial cultures (E and F) were infected with 1 PFU/cell of RA59, RJHM, or SeV or mock infected. At 24 h p.i., IFN-β mRNA (C and E) and mRNA7 (D and F) levels were measured by real-time qPCR. Real-time qPCR data are represented as the relative induction over mock-infected cells. Error bars represent the standard error of the mean of three replicates, and data are derived from one representative experiment of two.

cence intensity (MFI) of the IFN-β signal compared to mock-infected cells, with RA59 causing a slightly greater shift than RJHM. Importantly, the majority of cells, 85.2% of RA59-infected and 68.9% of RJHM-infected cells, exhibited positive staining for IFN-β compared with only 5.78% of mock-infected BMM. It should be noted that the fluorescence seen in mock-infected cells represents background fluorescence, consistent with manufacturer's product specifications. The magnitude of the positive shift in fluorescence seen with MHV-infection is also in agreement with product specifications. This result indicates that MHV induces the production of IFN-β protein in these BMM.

To further examine the cell types that contribute to the type I IFN response in the brains of MHV-infected animals, mononuclear cells were isolated from the brains of RA59- and RJHM-infected WT C57BL/6 mice at day 5 p.i. Brain-derived

mononuclear cells were surface stained for CD45, CD11b, CD11c, and CD3. Cells were then permeabilized, stained for intracellular expression of IFN-β, and analyzed by flow cytometry (Fig. 6). Cells were gated based on CD45 and CD11b expression, with CD11b^{hi} CD45^{hi} cells defined as macrophages and CD11b^{int} CD45^{int} cells defined as microglia (Fig. 6A), and examined for IFN-β expression (Fig. 6B and C). Consistent with previous results (14, 38, 39), MHV infection resulted in a significant infiltration of macrophages, with more being recruited during RJHM infection than with RA59 infection. While neither CD11c^{+} DCs nor CD3^{+} T cells expressed IFN-β in the brains of infected mice (data not shown), a higher percentage of CD11b^{hi} CD45^{hi} macrophages from RA59-infected (23.2%) and RJHM-infected (33.3%) brains expressed IFN-β than cells from mock-infected brains (14.6%) (Fig. 6B). Similar results were obtained for CD11b^{int} CD45^{int} microglia

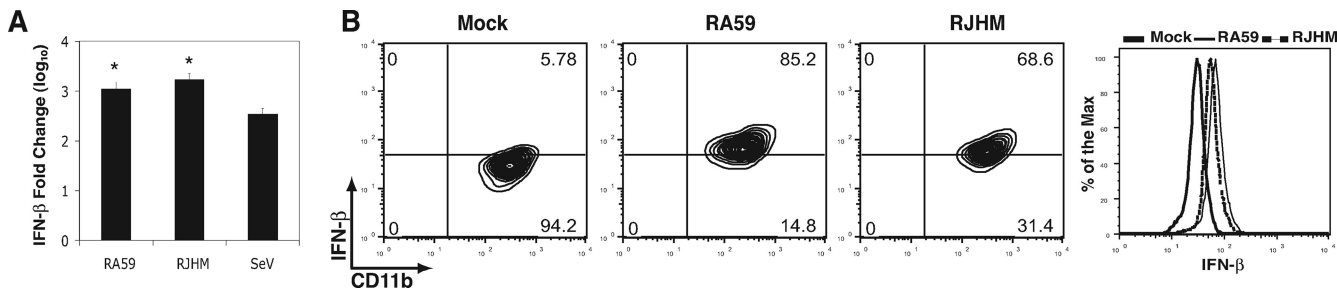

FIG. 5. IFN-β expression in primary BMM macrophages during MHV infection. (A) Primary BMM were infected with 0.5 PFU/cell of RA59, RJHM, or SeV or mock infected. At 24 h p.i., whole-cell RNA was isolated, and IFN-β mRNA levels were measured by real-time qPCR. Real-time qPCR data are represented as the relative induction over mock-infected cells. Error bars represent the standard error of the mean of three replicates, and data are derived from one representative experiment of two. Statistical analysis was performed using a Student's t test. *, P < 0.05. (B) BMM were infected with 0.5 PFU/cell of RA59 or RJHM. At 24 h p.i., cells were isolated, surface stained for CD11b and CD11c, and then stained for intracellular IFN-β for flow cytometric analysis. Contour plots and histograms represent CD11b^{+} CD11c^{−} cells.
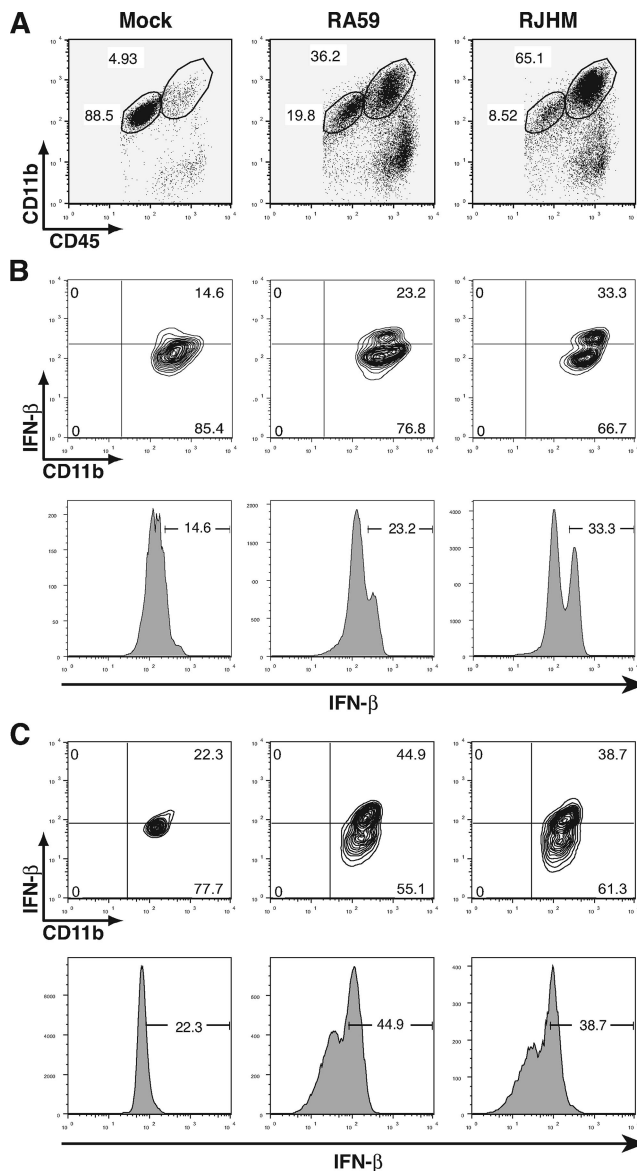
FIG. 6. IFN-β expression in brain-derived macrophages and microglia during MHV infection. Pooled brain-derived mononuclear cells were isolated from C57BL/6 mice infected i.c. with 500 PFU of RA59 ($n = 12$) or 10 PFU of RJHM ($n = 10$) or mock infected ($n = 14$) at day 5 p.i. Cells were surface stained for CD11b, CD11c, and CD45 and then stained for intracellular IFN-β for flow cytometric analysis. (A) Gating of CD11b^{+} CD45^{+} cells. FACS analysis was performed for CD11c^{−} CD11b^{hi} CD45^{hi} (B) and CD11c^{−} CD11b^{int} CD45^{int} (C) cells. Density plots and the corresponding histograms are from one representative experiment of four.

(Fig. 6C). A higher percentage of microglia from RA59-infected (44.9%) and RJHM-infected (38.7%) brains expressed IFN-β protein than cells from mock-infected brains (22.3%). Thus, infiltrating macrophages and resident microglia produce type I IFN in the brain during MHV infection. It should be noted that MHV infection resulted in a slight downward shift in the IFN-β signal, such that the MFI of the IFN-β-negative (IFN-β[−]) population of cells from MHV-infected brains was slightly lower than the MFI of cells from mock-infected brains.

While the mechanism behind this shift is unclear, we hypothesize that we are underestimating the percentage of IFN-β positive (IFN-β[+]) macrophages and microglia from MHV-infected samples and subsequently overestimating the percentage of IFN-β^{+} cells from mock-infected samples as there is little to no IFN-β protein in the brains of mock-infected animals (40).

MHV induces IFN-β in primary BMM by an MDA5-dependent pathway. To determine which PRR(s) is used for recognition of MHV in macrophages, primary BMM cultures were derived from WT C57BL/6, WT 129x1/SvJ, MyD88^{−/−} (C57BL/6 background), TLR3^{−/−} (C57BL/6 background), RIG-I^{−/−} (ICR × 129x1/SvJ × C57BL/6 background), and MDA5^{−/−} (129x1/SvJ background) mice. BMM were infected with RA59, RJHM, or SeV, and RNA was isolated at 24 h p.i. to measure IFN-β mRNA by real-time qPCR (Fig. 7). Expression of MyD88 (Fig. 7A) or TLR3 (Fig. 7B) was not necessary for the induction of IFN-β mRNA by either MHV or SeV. However, while MHV induction of IFN-β mRNA was independent of RIG-I in BMM, induction by SeV was significantly reduced in RIG-I^{−/−} BMM cultures (Fig. 7C). This is consistent with previous data showing that RIG-I is essential for type I IFN induction by SeV in mouse embryonic fibroblasts (MEFs) (19).

In contrast to IFN-β mRNA induction in WT 129x1/SvJ BMM cultures, neither RA59 nor RJHM was able to induce IFN-β gene transcription in the MDA5^{−/−} BMM cultures (Fig. 7D). This indicates that MHV induces a type I IFN response by an MDA5-dependent pathway in BMM. Interestingly, the ability of SeV to induce a type I IFN response was reduced in MDA5^{−/−} BMM cultures. This is consistent with recent data that suggest that MDA5 is involved in early recognition of SeV in MEFs (27) and DCs (56). To verify that the reduction of IFN-β mRNA in MDA5^{−/−} BMM cultures results in a decrease of IFN-β protein, an IFN bioassay was performed on the supernatants of infected BMM (Fig. 7F). While supernatants from MHV- or SeV-infected WT BMM were able to inhibit replication of the IFN-sensitive NDV, only supernatants from SeV-infected MDA5^{−/−} BMM inhibited replication of NDV, indicating that neither RA59 nor RJHM induced IFN-β protein production in these cells. Although IFN-β mRNA levels induced by SeV were reduced in the absence of MDA5, there was enough IFN-β mRNA present to make IFN-β protein, leading to inhibition of NDV replication. To ensure that RA59 and RJHM can replicate in MDA5^{−/−} BMM cultures, RNA was isolated at 24 h p.i., and mRNA7 levels were quantified by real-time qPCR (Fig. 7E). Both RA59 and RJHM could replicate to equivalent levels in WT and MDA5^{−/−} BMM cultures. Taken together, these data indicate that MDA5 is essential for the recognition of MHV and the subsequent induction of the type I IFN response in macrophages.

DISCUSSION

The type I IFN response represents a vital part of the innate immune system that forms the first line of defense against viral infection. Type I IFN plays a crucial role in reducing viral replication in vivo, as well as restricting the spread of the virus into organs that are not infected in immunocompetent WT
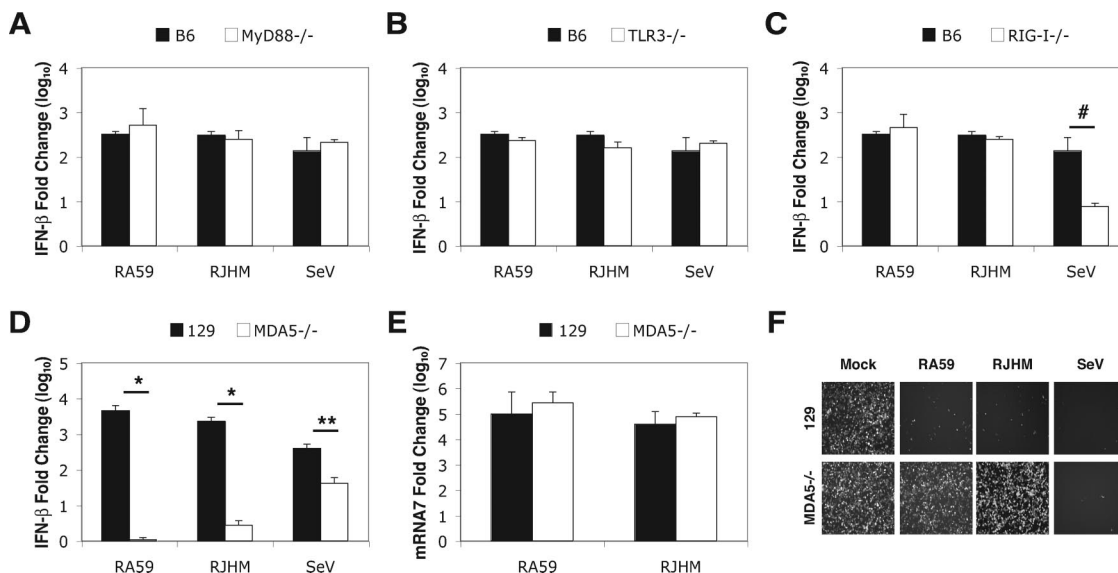
FIG. 7. IFN-β expression in MHV-infected primary BMM cultures isolated from WT and PRR knockout mice. Primary BMM cultures isolated from WT C57BL/6 (B6), WT 129x1/SvJ (129), MyD88$^{-/-}$, TLR3$^{-/-}$, RIG-I$^{-/-}$, and MDA5$^{-/-}$ mice were infected with 0.5 PFU/cell of RA59, RJHM, or SeV or mock infected. At 24 h p.i., whole-cell RNA was isolated, and IFN-β mRNA (A to D) and mRNA7 (E) levels were measured by real-time qPCR. Real-time qPCR data are represented as the relative induction over mock-infected cells. Error bars represent the standard error of the mean of three replicates. Statistical analysis was performed using a Student's t test. #, $P < 0.02$; *, $P < 0.00003$; **, $P < 0.004$. (F) Primary BMM cultures isolated from WT 129x1/SvJ and MDA5$^{-/-}$ mice were infected with 0.5 PFU/cell of RA59, RJHM, or SeV or mock infected. At 24 h p.i., supernatant was collected, subjected to UV radiation to inactive virus, and applied to L2 fibroblast cells for an IFN-β bioassay. At 24 h posttreatment, L2 cells were infected with 1 PFU/cell of NDV-GFP. NDV-GFP replication was visualized by fluorescence microscopy at 24 h p.i. Original magnification, ×40. All data are derived from one representative experiment of two.

mice (15, 28, 29, 42). Infection of IFNAR-deficient mice with the RA59 or RJHM strains of MHV by i.c. inoculation resulted in enhanced replication and tissue tropism compared to infection of WT mice. This is in agreement with previous studies examining MHV replication in IFNAR-deficient mice. Using an attenuated glial-tropic variant of JHM, JHM v2.2-1, Ireland et al. (16) showed increased susceptibility of IFNAR$^{-/-}$ mice and an increase in cellular tropism in the central nervous system (CNS) of these animals. In addition, intraperitoneal inoculation of IFNAR$^{-/-}$ mice with RA59 resulted in dissemination of the virus to the brain, spleen, and lungs and death by day 2 p.i. (7). Since the IFNAR$^{-/-}$ mice are also heterozygous at the IL-12R locus (IL-12R$^{+/-}$), congenic IL-12R$^{+/-}$ mice were infected to determine if this heterozygosity contributed to the increased viral replication in the IFNAR$^{-/-}$ mice. Viral replication and spread among organs in IL-12R$^{+/-}$ and WT C57BL/6 mice were the same (data not shown), indicating that the increased spread in the IFNAR$^{-/-}$ mice is due to the lack of a type I IFN response.

Interestingly, MHV induces the expression of IFN-β in the brains and livers of infected WT animals, both of which are principle targets of MHV replication. The neurotropic RA59 and RJHM strains of MHV induce IFN-β mRNA and protein expression in the brains of infected animals, and the hepatotropic strains (RA59, MHV-2, and MHV-3) induce IFN-β expression in the livers of infected animals, as measured by real-time qPCR and ELISA. While the type I IFN response appears to be sufficient to control spread to many organs, as demonstrated by the increased tissue tropism of MHV in mice deficient in IFNAR expression, it does not prevent replication of MHV in the brains and livers of WT mice.

While it is unclear why type I IFN can restrict MHV spread to some organs but not others, there is evidence that treatment of MHV-infected athymic mice with recombinant IFN-β after an infection has been established is ineffective in controlling disease progression; however, treatment prior to infection can protect the mouse from disease (46). Therefore, it is possible that MHV is able to establish a robust infection in certain organs, such as the brain and the liver, before the type I IFN response is induced. Even if type I IFN is induced, MHV has already replicated to a high enough level that it overwhelms the effects of the type I IFN response. In addition, there is evidence that some cell types are "prearmed" with basal levels of IFN-β expression and are therefore resistant to viral infection. In a study of cardiac antiviral responses during reovirus infection, Zurney et al. (59) found that cardiac myocytes expressed basal levels of IFN-β and were protected against viral infection. Thus, it is possible that cells in organs outside of the typical MHV targets may be primed with basal expression of type I IFN, and MHV is therefore unable to establish an infection.

While primary cultured neurons and astrocytes do not produce IFN-β in response to MHV infection, microglial cultures expressed high levels of IFN-β mRNA in response to MHV infection. Since microglia are macrophage-like cells, we investigated whether another population of macrophages, primary BMM, also secreted IFN-β in response to MHV. These cells also produced IFN-β mRNA and IFN-β protein in response to MHV infection, as determined by real-time qPCR and fluorescence-activated cell sorting (FACS) analysis.

To examine the ability of inflammatory macrophages and resident microglia in the CNS of infected mice to express

IFN-β and to determine if other immune cells produce IFN-β during MHV infection of the CNS, we isolated brain-derived mononuclear cells and subjected them to intracellular IFN-β staining and FACS analysis. CD11c$^+$ DCs did not express IFN-β protein in MHV-infected brains (data not shown), in agreement with previous data showing that MHV is unable to induce type I IFN production in conventional DCs (7, 58). In addition, CD3$^+$ T cells did not express IFN-β protein (data not shown). However, CD11b^{hi} CD45^{hi} macrophages and CD11b^{int} CD45^{int} cells from MHV-infected brains expressed IFN-β protein.

Microglia play a crucial role during MHV pathogenesis in the CNS. Using the attenuated variant of JHM, JHM v2.2-1, that causes a demyelinating disease similar to RA59, studies have shown that major histocompatibility complex class I is upregulated on activated microglia in MHV-infected animals (4, 16). Major histocompatibility complex class I upregulation is dependent upon type I IFN, and the authors suggest that this is crucial for optimizing antigen presentation in the CNS during early infection with MHV (16). In addition, macrophages comprise a major component of inflammatory cells contributing to the innate immune response in the CNS as well as to the CNS pathology during acute MHV encephalitis (38, 39). The data presented here suggest that one mechanism by which macrophages contribute to host protection is through secretion of type I IFN.

This is the first study to demonstrate type I IFN induction by MHV in cells other than pDCs, the major IFN-α-producing cells in vivo. Cervantes-Barragan et al. (7) demonstrated that pDCs rapidly produce high levels of IFN-α in response to MHV. Furthermore, this was necessary for control of virus replication as pDC depletion led to significant increases in viral replication in several organs, though levels did not reach the levels of viral replication observed in IFNAR-deficient mice (7, 58). However, IFN-α mRNA levels were below the level of detection in the brains and livers of MHV-infected animals (data not shown). Therefore, while pDCs likely play an important role in controlling MHV replication, the results obtained herein indicate that they are not the only source of type I IFN during MHV infection. We show here that macrophages and macrophage-like microglia contribute to the type I IFN response in MHV-infected animals.

Type I IFN induction by macrophages during viral infection plays an important role in shaping the pathogenesis of several viruses. Mopeia virus, along with herpes simplex virus types I and II (30), induces type I IFN expression in monocyte-derived macrophages, which may play an important role in controlling early viral replication in vivo (32). In addition, intranasal infection with NDV leads to the rapid expression of IFN-α in alveolar macrophages in vivo (23), suggesting that type I IFN expression is important for early control of NDV replication. Notably, SARS-CoV can induce the expression of type I IFN in human peripheral macrophages (53), suggesting that other CoVs may induce type I IFN in a cell type similar to MHV.

The lack of IFN-β induction in primary hepatocytes following MHV infection suggests that this cell type is probably not responsible for MHV-induced type I IFN in the liver. However, cultured primary cells may not completely reflect gene expression of hepatocytes in vivo, so hepatocytes cannot be completely ruled out as a source of IFN-β in vivo. Although hepatocytes are the major parenchymal cells in the liver, the liver sinusoidal endothelial cells and the macrophage-like Kupffer cells (KCs) are the important immune cells in the liver, playing a crucial role in antigen uptake and presentation (21). While we have thus far been unable to identify the IFN-producing cells in the liver, our results from analysis of IFN-producing cells in the brain suggest that KCs are likely the IFN-producing cells of the liver. In fact, KCs are the largest population of macrophages in the body (21).

Viruses are recognized by PRRs that reside on the plasma membrane or in endosomes (TLRs) or in the cytoplasm (RIG-I and MDA5). Typically, RNA viruses produce dsRNA and are therefore recognized by either RIG-I or MDA5. Both RIG-I and MDA5 contain an RNA helicase domain, which binds to dsRNA, and a caspase recruitment domain that is required to bind the adaptor IPS-1 (IFN-β promoter stimulator 1). When bound to dsRNA, RIG-I and MDA5 can bind to IPS-1, which resides in the mitochondrial membrane, resulting in the transmission of signals that lead to the activation of IRF-3 and the production of IFN-β (24, 54, 55). Recent data have suggested that RIG-I recognizes not only small dsRNA moieties (18) but also single-stranded RNA containing 5′ triphosphates (12, 13, 36), usually found on the genomes of negative-strand RNA viruses. MDA5 appears to recognize long dsRNA moieties (18), including polyriboinosinic-polyribocytidylic acid (10, 19), while it does not recognize RNA containing 5′ triphosphates.

Quantification of IFN-β mRNA levels in a panel of MHV-infected primary BMM deficient in various PRRs indicates that MHV is recognized by MDA5 and that MDA5 is necessary for IFN-β mRNA induction following MHV infection in these cells. While MHV induced equivalent amounts of IFN-β in MyD88$^{-/-}$, TLR3$^{-/-}$, and RIG-I$^{-/-}$ BMM cultures, IFN-β production was almost completely ablated in MDA5$^{-/-}$ BMM cultures, indicating that MDA5 is essential to the recognition of MHV in these cells. While viruses in the rhabdovirus, paramyxovirus, orthomyxovirus, and flavivirus families have been shown to be recognized primarily by RIG-I, only members of the picornavirus family have been shown to induce type I IFN by a strictly MDA5-dependent pathway prior to this study (10, 19, 27). Thus, this is the first study to demonstrate the use of MDA5 as the main PRR for a family of viruses other than picornaviruses. It is not surprising that MHV is recognized by MDA5 and not by RIG-I as both the genomic mRNA and subgenomic mRNAs generated during MHV replication contain a 5′ methylated cap (25), similar to host cell mRNAs, blocking recognition of the 5′ triphosphate moiety. As MHV generates ample amounts of dsRNA during replication (47), it is likely that MDA5 senses this dsRNA, leading to the production of type I IFN. It should be noted, however, that MHV induces IFN-α expression by a TLR7-dependent mechanism in pDCs (7), as is common for IFN induction in pDCs. It is unclear why MHV is able to induce type I IFN expression in macrophages and microglia but not in other primary cell types, as shown in this study, or in L2 fibroblast cells (40) or other immortalized cell lines (9, 47, 48, 57). However, preliminary data suggest that MDA5 mRNA expression levels are significantly lower in L2 fibroblast cells and in some primary cell types, including neurons, than in macrophages (data not shown). This suggests that the level of MDA5 mRNA ex-

pressed in uninfected cells is one factor that determines whether MHV infection results in type I IFN induction in a particular cell type. Future work will be directed at further understanding the recognition of MHV by MDA5.

REFERENCES

1. Adachi, O., T. Kawai, K. Takeda, M. Matsumoto, H. Tsutsui, M. Sakagami, K. Nakanishi, and S. Akira. 1998. Targeted disruption of the MyD88 gene results in loss of IL-1- and IL-18-mediated function. Immunity 9:143–150.
2. Alexopoulou, L., A. C. Holt, R. Medzhitov, and R. A. Flavell. 2001. Recognition of double-stranded RNA and activation of NF-κB by Toll-like receptor 3. Nature 413:732–738.
3. Basler, C. F., A. Mikulasova, L. Martinez-Sobrido, J. Paragas, E. Muhlberger, M. Bray, H. D. Klenk, P. Palese, and A. Garcia-Sastre. 2003. The Ebola virus VP35 protein inhibits activation of interferon regulatory factor 3. J. Virol. 77:7945–7956.
4. Bergmann, C. C., B. Parra, D. R. Hinton, R. Chandran, M. Morrison, and S. A. Stohlman. 2003. Perforin-mediated effector function within the central nervous system requires IFN-gamma-mediated MHC up-regulation. J. Immunol. 170:3204–3213.
5. Burnham, A. J., L. Gong, and R. W. Hardy. 2007. Heterogeneous nuclear ribonuclear protein K interacts with Sindbis virus nonstructural proteins and viral subgenomic mRNA. Virology 367:212–221.
6. Caamano, J., J. Alexander, L. Craig, R. Bravo, and C. A. Hunter. 1999. The NF-κB family member RelB is required for innate and adaptive immunity to Toxoplasma gondii. J. Immunol. 163:4453–4461.
7. Cervantes-Barragan, L., R. Zust, F. Weber, M. Spiegel, K. S. Lang, S. Akira, V. Thiel, and B. Ludewig. 2007. Control of coronavirus infection through plasmacytoid dendritic cell-derived type I interferon. Blood 109:1131–1137.
8. Garcia-Sastre, A., and C. A. Biron. 2006. Type 1 interferons and the virus-host relationship: a lesson in detente. Science 312:879–882.
9. Garlinghouse, L. E., Jr., A. L. Smith, and T. Holford. 1984. The biological relationship of mouse hepatitis virus (MHV) strains and interferon: in vitro induction and sensitivities. Arch. Virol. 82:19–29.
10. Gitlin, L., W. Barchet, S. Gilfillan, M. Cella, B. Beutler, R. A. Flavell, M. S. Diamond, and M. Colonna. 2006. Essential role of mda-5 in type I IFN responses to polyriboinosinic:polyribocytidylic acid and encephalomyocarditis picornavirus. Proc. Natl. Acad. Sci. USA 103:8459–8464.
11. Gombold, J. L., S. T. Hingley, and S. R. Weiss. 1993. Fusion-defective mutants of mouse hepatitis virus A59 contain a mutation in the spike protein cleavage signal. J. Virol. 67:4504–4512.
12. Habjan, M., I. Andersson, J. Klingstrom, M. Schumann, A. Martin, P. Zimmermann, V. Wagner, A. Pichlmair, U. Schneider, E. Muhlberger, A. Mirazimi, and F. Weber. 2008. Processing of genome 5′ termini as a strategy of negative-strand RNA viruses to avoid RIG-I-dependent interferon induction. PLoS ONE 3:e2032.
13. Hornung, V., J. Ellegast, S. Kim, K. Brzozka, A. Jung, H. Kato, H. Poeck, S. Akira, K. K. Conzelmann, M. Schlee, S. Endres, and G. Hartmann. 2006. 5′-Triphosphate RNA is the ligand for RIG-I. Science 314:994–997.
14. Iacono, K. T., L. Kazi, and S. R. Weiss. 2006. Both spike and background genes contribute to murine coronavirus neurovirulence. J. Virol. 80:6834–6843.
15. Ida-Hosonuma, M., T. Iwasaki, T. Yoshikawa, N. Nagata, Y. Sato, T. Sata, M. Yoneyama, T. Fujita, C. Taya, H. Yonekawa, and S. Koike. 2005. The alpha/beta interferon response controls tissue tropism and pathogenicity of poliovirus. J. Virol. 79:4460–4469.
16. Ireland, D. D., S. A. Stohlman, D. R. Hinton, R. Atkinson, and C. C. Bergmann. 2008. Type I interferons are essential in controlling neurotropic coronavirus infection irrespective of functional CD8 T cells. J. Virol. 82:300–310.
17. Kamitani, W., K. Narayanan, C. Huang, K. Lokugamage, T. Ikegami, N. Ito, H. Kubo, and S. Makino. 2006. Severe acute respiratory syndrome corona-
18. virus Nsp1 protein suppresses host gene expression by promoting host mRNA degradation. Proc. Natl. Acad. Sci. USA 103:12885–12890.
18. Kato, H., O. Takeuchi, E. Mikamo-Satoh, R. Hirai, T. Kawai, K. Matsushita, A. Hiiragi, T. S. Dermody, T. Fujita, and S. Akira. 2008. Length-dependent recognition of double-stranded ribonucleic acids by retinoic acid-inducible gene-I and melanoma differentiation-associated gene 5. J. Exp. Med. 205:1601–1610.
19. Kato, H., O. Takeuchi, S. Sato, M. Yoneyama, M. Yamamoto, K. Matsui, S. Uematsu, A. Jung, T. Kawai, K. J. Ishii, O. Yamaguchi, K. Otsu, T. Tsujimura, C. S. Koh, C. Reis e Sousa, Y. Matsuura, T. Fujita, and S. Akira. 2006. Differential roles of MDA5 and RIG-I helicases in the recognition of RNA viruses. Nature 441:101–105.
20. Katze, M. G., Y. He, and M. Gale, Jr. 2002. Viruses and interferon: a fight for supremacy. Nat. Rev. Immunol. 2:675–687.
21. Knolle, P. A., and G. Gerken. 2000. Local control of the immune response in the liver. Immunol. Rev. 174:21–34.
22. Kopecky-Bromberg, S. A., L. Martinez-Sobrido, M. Frieman, R. A. Baric, and P. Palese. 2007. Severe acute respiratory syndrome coronavirus open reading frame (ORF) 3b, ORF 6, and nucleocapsid proteins function as interferon antagonists. J. Virol. 81:548–557.
23. Kumagai, Y., O. Takeuchi, H. Kato, H. Kumar, K. Matsui, E. Morii, K. Aozasa, T. Kawai, and S. Akira. 2007. Alveolar macrophages are the primary interferon-alpha producer in pulmonary infection with RNA viruses. Immunity 27:240–252.
24. Kumar, H., T. Kawai, H. Kato, S. Sato, K. Takahashi, C. Coban, M. Yamamoto, S. Uematsu, K. J. Ishii, O. Takeuchi, and S. Akira. 2006. Essential role of IPS-1 in innate immune responses against RNA viruses. J. Exp. Med. 203:1795–1803.
25. Lai, M. M., C. D. Patton, and S. A. Stohlman. 1982. Further characterization of mRNA's of mouse hepatitis virus: presence of common 5′-end nucleotides. J. Virol. 41:557–565.
26. Lavi, E., A. Suzumura, M. Hirayama, M. K. Highkin, D. M. Dambach, D. H. Silberberg, and S. R. Weiss. 1987. Coronavirus mouse hepatitis virus (MHV)-A59 causes a persistent, productive infection in primary glial cell cultures. Microb. Pathog. 3:79–86.
27. Loo, Y. M., J. Fornek, N. Crochet, G. Bajwa, O. Perwitasari, L. Martinez-Sobrido, S. Akira, M. A. Gill, A. Garcia-Sastre, M. G. Katze, and M. Gale, Jr. 2008. Distinct RIG-I and MDA5 signaling by RNA viruses in innate immunity. J. Virol. 82:335–345.
28. Luker, G. D., J. L. Prior, J. Song, C. M. Pica, and D. A. Leib. 2003. Bioluminescence imaging reveals systemic dissemination of herpes simplex virus type 1 in the absence of interferon receptors. J. Virol. 77:11082–11093.
29. Luker, K. E., M. Hutchens, T. Schultz, A. Pekosz, and G. D. Luker. 2005. Bioluminescence imaging of vaccinia virus: effects of interferon on viral replication and spread. Virology 341:284–300.
30. Malmgaard, L., J. Melchjorsen, A. G. Bowie, S. C. Mogensen, and S. R. Paludan. 2004. Viral activation of macrophages through TLR-dependent and -independent pathways. J. Immunol. 173:6890–6898.
31. Navas, S., and S. R. Weiss. 2003. Murine coronavirus-induced hepatitis: JHM genetic background eliminates A59 spike-determined hepatotropism. J. Virol. 77:4972–4978.
32. Pannetier, D., C. Faure, M. C. Georges-Courbot, V. Deubel, and S. Baize. 2004. Human macrophages, but not dendritic cells, are activated and produce alpha/beta interferons in response to Mopeia virus infection. J. Virol. 78:10516–10524.
33. Park, M. S., M. L. Shaw, J. Munoz-Jordan, J. F. Cros, T. Nakaya, N. Bouvier, P. Palese, A. Garcia-Sastre, and C. F. Basler. 2003. Newcastle disease virus (NDV)-based assay demonstrates interferon-antagonist activity for the NDV V protein and the Nipah virus V, W, and C proteins. J. Virol. 77:1501–1511.
34. Phillips, J. J., M. M. Chua, E. Lavi, and S. R. Weiss. 1999. Pathogenesis of chimeric MHV4/MHV-A59 recombinant viruses: the murine coronavirus spike protein is a major determinant of neurovirulence. J. Virol. 73:7752–7760.
35. Phillips, J. J., M. M. Chua, G. F. Rall, and S. R. Weiss. 2002. Murine coronavirus spike glycoprotein mediates degree of viral spread, inflammation, and virus-induced immunopathology in the central nervous system. Virology 301:109–120.
36. Pichlmair, A., O. Schulz, C. P. Tan, T. I. Naslund, P. Liljestrom, F. Weber, and C. Reis e Sousa. 2006. RIG-I-mediated antiviral responses to single-stranded RNA bearing 5′-phosphates. Science 314:997–1001.
37. Platanias, L. C. 2005. Mechanisms of type-I- and type-II-interferon-mediated signalling. Nat. Rev. Immunol. 5:375–386.
38. Rempel, J. D., S. J. Murray, J. Meisner, and M. J. Buchmeier. 2004. Differential regulation of innate and adaptive immune responses in viral encephalitis. Virology 318:381–392.
39. Rempel, J. D., S. J. Murray, J. Meisner, and M. J. Buchmeier. 2004. Mouse hepatitis virus neurovirulence: evidence of a linkage between S glycoprotein expression and immunopathology. Virology 318:45–54.
40. Roth-Cross, J. K., L. Martinez-Sobrido, E. P. Scott, A. Garcia-Sastre, and S. R. Weiss. 2007. Inhibition of the alpha/beta interferon response by mouse hepatitis virus at multiple levels. J. Virol. 81:7189–7199.

41. **Samuel, C. E.** 2001. Antiviral actions of interferons. Clin. Microbiol. Rev. **14:**778–809.

42. **Samuel, M. A., and M. S. Diamond.** 2005. Alpha/beta interferon protects against lethal West Nile virus infection by restricting cellular tropism and enhancing neuronal survival. J. Virol. **79:**13350–13361.

43. **Sarma, J. D., L. Fu, S. T. Hingley, and E. Lavi.** 2001. Mouse hepatitis virus type-2 infection in mice: an experimental model system of acute meningitis and hepatitis. Exp. Mol. Pathol. **71:**1–12.

44. **Skinner, M. A., and S. G. Siddell.** 1983. Coronavirus JHM: nucleotide sequence of the mRNA that encodes nucleocapsid protein. Nucleic Acids Res. **11:**5045–5054.

45. **Taguchi, F., and S. G. Siddell.** 1985. Difference in sensitivity to interferon among mouse hepatitis viruses with high and low virulence for mice. Virology **147:**41–48.

46. **Uetsuka, K., H. Nakayama, and N. Goto.** 1996. Protective effect of recombinant interferon (IFN)-α/β on MHV-2cc-induced chronic hepatitis in athymic nude mice. Exp. Anim. **45:**293–297.

47. **Versteeg, G. A., P. J. Bredenbeek, S. H. van den Worm, and W. J. Spaan.** 2007. Group 2 coronaviruses prevent immediate early interferon induction by protection of viral RNA from host cell recognition. Virology **361:**18–26.

48. **Versteeg, G. A., O. Slobodskaya, and W. J. Spaan.** 2006. Transcriptional profiling of acute cytopathic murine hepatitis virus infection in fibroblast-like cells. J. Gen. Virol. **87:**1961–1975.

49. **Virelizier, J. L., and A. C. Allison.** 1976. Correlation of persistent mouse hepatitis virus (MHV-3) infection with its effect on mouse macrophage cultures. Arch. Virol. **50:**279–285.

50. **Wathelet, M. G., M. Orr, M. B. Frieman, and R. S. Baric.** 2007. Severe acute respiratory syndrome coronavirus evades antiviral signaling: role of Nsp1 and rational design of an attenuated strain. J. Virol. **81:**11620–11633.

51. **Weiss, S. R., and S. Navas-Martin.** 2005. Coronavirus pathogenesis and the emerging pathogen severe acute respiratory syndrome coronavirus. Microbiol. Mol. Biol. Rev. **69:**635–664.

52. **Ye, Y., K. Hauns, J. O. Langland, B. L. Jacobs, and B. G. Hogue.** 2007. Mouse hepatitis coronavirus A59 nucleocapsid protein is a type I interferon antagonist. J. Virol. **81:**2554–2563.

53. **Yilla, M., B. H. Harcourt, C. J. Hickman, M. McGrew, A. Tamin, C. S. Goldsmith, W. J. Bellini, and L. J. Anderson.** 2005. SARS-coronavirus replication in human peripheral monocytes/macrophages. Virus Res. **107:**93–101.

54. **Yoneyama, M., M. Kikuchi, K. Matsumoto, T. Imaizumi, M. Miyagishi, K. Taira, E. Foy, Y. M. Loo, M. Gale, Jr., S. Akira, S. Yonehara, A. Kato, and T. Fujita.** 2005. Shared and unique functions of the DExD/H-box helicases RIG-I, MDA5, and LGP2 in antiviral innate immunity. J. Immunol. **175:**2851–2858.

55. **Yoneyama, M., M. Kikuchi, T. Natsukawa, N. Shinobu, T. Imaizumi, M. Miyagishi, K. Taira, S. Akira, and T. Fujita.** 2004. The RNA helicase RIG-I has an essential function in double-stranded RNA-induced innate antiviral responses. Nat. Immunol. **5:**730–737.

56. **Yount, J. S., L. Gitlin, T. M. Moran, and C. B. Lopez.** 2008. MDA5 participates in the detection of paramyxovirus infection and is essential for the early activation of dendritic cells in response to Sendai virus defective interfering particles. J. Immunol. **180:**4910–4918.

57. **Zhou, H., and S. Perlman.** 2007. Mouse hepatitis virus does not induce beta interferon synthesis and does not inhibit its induction by double-stranded RNA. J. Virol. **81:**568–574.

58. **Zhou, H., and S. Perlman.** 2006. Preferential infection of mature dendritic cells by mouse hepatitis virus strain JHM. J. Virol. **80:**2506–2514.

59. **Zurney, J., K. E. Howard, and B. Sherry.** 2007. Basal expression levels of IFNAR and Jak-STAT components are determinants of cell-type-specific differences in cardiac antiviral responses. J. Virol. **81:**13668–13680.

60. **Zust, R., L. Cervantes-Barragan, T. Kuri, G. Blakqori, F. Weber, B. Ludewig, and V. Thiel.** 2007. Coronavirus nonstructural protein 1 is a major pathogenicity factor: implications for the rational design of coronavirus vaccines. PLoS Pathog. **3:**e109.